石油科学通报
Petroleum Science Bulletin

纳米颗粒球形度对倾斜通道中纳米流体反向混合对流传热的影响

尤翔程*，李世远

中国石油大学(北京)石油工程学院，北京 102249
* 通信作者, xcyou@cup.edu.cn

收稿日期: 2021−05−07
国家自然科学基金(12002390)、国家自然科学基金(51704307) 和中国石油大学(北京) 科研基金资助(ZX20200119) 联合资助

摘要　本文研究了纳米颗粒球形度对倾斜通道中纳米流体反向混合对流传热的影响，以及不同纳米颗粒球形度和纳米颗粒体积分数对流体流动和传热的基本参数的影响。本文将控制常微分方程无量纲化，解析求解，得到了速度、温度和压力的显式分布。纳米流体的流动反转、壁面平均摩擦系数和平均努赛尔数对纳米流体的影响取决于纳米颗粒球形度，纳米颗粒体积分数和压力参数等。结果表明，纳米颗粒的体积分数在延迟逆流发生方面起着关键作用。纳米流体比基础流体具有更大的延迟范围，约为基础流体的 2.2 倍。同时，随着纳米颗粒球形度增大，其值也相应增大。纳米颗粒体积分数对速度和温度分布的影响是显著的，随着其值增大，与基液相比纳米流体延迟了上下壁面附近的速度降低。同时，随着纳米颗粒球形度的增大，壁面温度也降低。随着纳米颗粒的体积分数增大，纳米流体的壁面平均摩擦系数也增大，而且与纳米颗粒球形度和无量纲压力参数 P_2 均无关，随着 P_1 的增大而单调减小。平均努塞尔数与纳米颗粒球形度，纳米颗粒的体积分数和无量纲压力参数 P_2 均有关。随着纳米颗粒球形度的增大，平均努塞尔数值也增大。本文对纳米微球在石油工程提高采收率中的应用进行了梳理和分析，深入研究纳米颗粒在倾斜通道中反向混合对流的传输机理，研究不同纳米颗粒球形度和纳米颗粒体积分数对流体流动和传热的物理参数的影响，可以为后续提高采收率纳米微球的参数选择提供理论支撑。

关键词　纳米颗粒球形度；倾斜通道；纳米流体；混合对流

Effect of nanoparticle sphericity on mixed convective flow of nanofluids in an inclined channel

YOU Xiangcheng, LI Shiyuan

College of Petroleum Engineering, China University of Petroleum-Beijing, Beijing 102249, China

Abstract　We studied the effect of nanoparticle sphericity on the mixed convective flow of nanofluids in an inclined channel, and the influence of different nanoparticle sphericity and nanoparticle volume fraction on the physical parameters of fluid flow and heat transfer has also been presented. The governing ordinary differential equations are dimensionless and solved analytically. The explicit distributions of velocity, temperature and pressure are obtained. The effect of the flow reversal of the nanofluid, the average wall friction coefficient and the average Nusselt number of the nanofluid depends on the nanoparticle

引用格式：尤翔程, 李世远. 纳米颗粒球形度对倾斜通道中纳米流体反向混合对流传热的影响. 石油科学通报, 2021, 04: 604−613
YOU Xiangcheng, LI Shiyuan. Effect of nanoparticle sphericity on mixed convective flow of nanofluids in an inclined channel. Petroleum Science Bulletin, 2021, 04: 604-613. doi: 10.3969/j.issn.2096-1693.2021.04.042

sphericity, the nanoparticle volume fraction and the pressure parameters. The results show that the volume fraction of nanoparticles plays a key role in delaying the occurrence of countercurrent flow. The nanofluid has a larger delay range , about 2.2 times that of the base fluid. At the same time, the value of nanoparticles increases with the increase of sphericity. The effect of nanoparticle volume fraction on velocity and temperature distribution is significant. With the increase of its value, the nanofluid delays the velocity reduction near the upper and lower walls compared with the base fluid. At the same time, the wall temperature decreases with an increase of the sphericity of nanoparticles. With an increase of the volume fraction of nanoparticles, the average wall friction coefficient of the nanofluid increases. This is independent of the sphericity of nanoparticles and the dimensionless pressure parameter P_2, and decreases monotonically with an increase of P_1. The average Nusselt number is related to the sphericity of nanoparticles, the volume fraction of nanoparticles and the dimensionless pressure parameter P_2. With an increase of the sphericity of nanoparticles, the average Nusselt value also increases. This paper analyzes the application of nano microspheres in petroleum engineering, studies the transfer mechanism of mixed convection of nano particles in inclined channels, and analyzes the effects of different nano particle sphericity and nano particle volume fraction on the physical parameters of fluid flow and heat transfer. It can provide theoretical support for subsequent parameter selection of nanospheres in enhanced oil recovery.

Keywords nanoparticle sphericity; inclined channel; nanofluids; mixed convection

doi: 10.3969/j.issn.2096-1693.2021.04.042

0 引言

众所周知，CHOI等[1]于1995年首先提出了纳米流体的概念；它们是在基础流体(例如乙二醇、油或水)中以一定的方式和比例添加纳米颗粒形成的悬浮液。相较于其他常规流体，纳米流体具备更多新颖特性，这使得纳米流体具有广阔的应用前景[2]。随着学科之间的交叉发展，纳米技术在食品、生物医学、电子、材料等行业的创新应用越来越受到关注。

石油大都储藏在地底深处多孔岩石中，纳米材料能够在纳米级岩石孔隙中自由流动，在改变储层岩石流变性和润湿性中显示出了很好的效果[3-4]。纳米粒子可以作为钻完井液添加剂，有助于改善流体的基础性能以及提高井筒完整性[5]。石油作为我国的一大战略储备能源，进一步加强纳米流体在石油工程中的基础性研究与应用具有重要意义[6-9]。除了固井[10-11]和油井增产[12-13]等，纳米技术或纳米颗粒在石油和天然气行业的其他应用也得到了广泛的研究，例如钻井液[14-15]和提高石油采收率[16-17]。在石油和天然气行业各领域开展纳米粒子研究情况如图1所示。可以看到，纳米粒子在提高采收率应用领域有广泛研究。

1 应用现状及前景分析

提高石油采收率工艺的主要目标是改变流体或岩石特性，以降低注水后残余油的含油饱和度。尽管纳米技术本身不是提高采收率技术，但纳米尺度上发现的特性可以改进当前提高采收率方法的性能，通过优化参数，最终提高石油采收率。

近年来，纳米聚合物微球调驱技术越来越受到关注[18-20]，具有良好的调驱效果及应用前景。纳米聚合物微球主要是由水溶性单体聚合形成的圆球状凝胶颗粒，粒径范围在纳米至微米级。纳米聚合物微球具有良好的吸水膨胀性能，运移过程中，单个大粒径微球膨胀后封堵孔喉，压力作用下，众多小粒径微球在孔喉中不断发生水化膨胀、封堵、形变，聚集堆积封堵高渗地层，实现较大幅度调整水驱流场，提高驱替剂波及系数，进而提高采收率。国内外关于聚合物微球的室内实验研究采用不同单体制备聚合物微球，并着重研究耐温耐盐性、溶胀性能、封堵性能和驱替性能[21-26]。聚合物微球在国内外油田也开展了相关的先

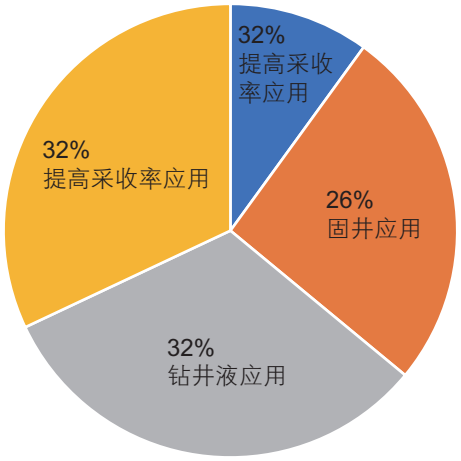

图1 在石油和天然气行业中纳米粒子研究的所占百分比

Fig. 1 Percentage of the investigations of nanoparticles in the oil and gas industry

导试验应用[27–30]。其中，文献[25]提出了一种智能化的纳米三次采油工艺，该工艺可实现从同步到连续的纳米三次采油的转变。在测试岩心上获得的结果显示，根据岩石性质，水驱采收率在 48%~63%，而智能纳米三次采油的最终采收率分别为 57%~85%。当基于岩石和流体性质对特定机理进行优化时，可对智能纳米提高采收率工艺进行参数微调，如体积、纳米粒子类型和所使用的注入机制，以达到最终采收率。因此，了解纳米微球的传输机理对其应用至关重要。

关于通道内的流体流动和传热问题，与基础流体相比，纳米流体显示出更多的热传递，如黏度、扩散系数、传热速率和导热系数等[31–35]。以往的研究大多集中在水平或垂直通道上[36–48]，其中文献[36–40]只考虑流体在通道内的流动和传热，没有考虑温度和纳米颗粒粒径的影响。国内外许多研究人员对不同纳米颗粒，如 Al_2O_3-H_2O 纳米流体、CuO-H_2O 纳米流体、Fe_3O_4-H_2O 纳米流体等在微小通道中对流传热问题进行了深入的数值模拟或实验研究[41–48]。目前国内外对倾斜几何结构中纳米流体的混合对流相对来说研究较少[49–55]，并且上述这些模型几乎没有考虑温度和纳米颗粒粒径的影响。深入研究纳米颗粒在通道中的传输机理，对于纳米流体在石油开采中的应用，既是当前亟待解决的基础理论研究难题，下一步对于石油领域纳米微球调驱、封堵技术，提高采收率等工程应用具有十分重要的意义。

2 数学模型

本文主要解析研究纳米颗粒球形度对倾斜通道中纳米流体反向混合对流传热的影响，研究不同纳米颗粒球形度和纳米颗粒体积分数对流体流动和传热的物理参数的影响。

考虑由浮力和外部压力梯度驱动的稳态混合对流，该压力梯度位于充满纳米流体的两平行倾斜通道之间，且间隔距离为 L。如图 2 显示了物理模型和坐标系，其中 x 轴沿下壁面向下，y 轴垂直于下壁面，q 是恒定壁面热流，g 是重力，γ 是两平行通道的倾斜角。在这种情况下，速度场由 $\boldsymbol{v}(u,0)$ 给出，连续性方程简化为 $\partial u/\partial x=0$，表示为 $u=u(y)$。参考 LAVINE[49]，使用纳米流体模型，根据 Boussinesq 近似，动量平衡和能量方程如下：

$$\frac{\partial p}{\partial x}=-(\rho\beta)_{nf}\,g(T-T_0)\sin\gamma+\mu_{nf}\frac{\partial^2 u}{\partial y^2}, \tag{1}$$

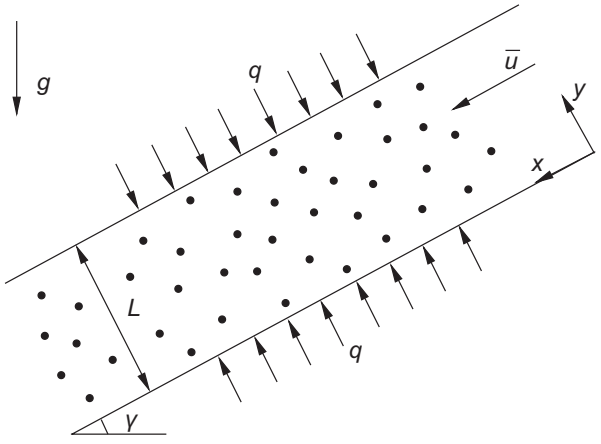

图 2 物理模型和坐标系

Fig. 2 Physical configuration and coordinate system

$$\frac{\partial p}{\partial y}=(\rho\beta)_{nf}\,g(T-T_0), \tag{2}$$

$$u\frac{\partial T}{\partial x}=\alpha_{nf}\frac{\partial^2 T}{\partial y^2}, \tag{3}$$

其边界条件为：

$$u(0)=u(L)=0,-\left.\frac{\partial T}{\partial y}\right|_{y=0}=\left.\frac{\partial T}{\partial y}\right|_{y=L}=1. \tag{4}$$

假设质量流量为本文倾斜通道流量研究的规定量，则该截面中的平均流速为

$$\bar{u}=\int_0^L u(y)\,\mathrm{d}y. \tag{5}$$

其中 u 是沿 x 轴的速度分量，$\bar{u}$ 是平均速度，T 是纳米流体温度，T_0 是恒定参考温度，p 是流体热力学压力，g 是重力加速度。注意，式(5)仅限于研究纳米颗粒的球形度，不考虑纳米颗粒的其他形状。

引入以下无量纲变量

$$P(X,Y)=\left[p-\rho_f g(x\sin\gamma-y\cos\gamma)\right]/\left(Pr\rho_f\bar{u}^2\right), \tag{6}$$

其中 L 是特征长度，$Pr=\nu_f/\alpha_f$ 是普朗特数。利用上述变量，控制方程转化为无量纲形式

$$\frac{\partial P}{\partial X}=-P_1\frac{(\rho\beta)_{nf}}{(\rho\beta)_f}\theta+\frac{\mu_{nf}}{\mu_f}\frac{\partial^2 U}{\partial Y^2}, \tag{7}$$

$$\frac{\partial P}{\partial Y}=P_2\frac{(\rho\beta)_{nf}}{(\rho\beta)_f}\theta, \tag{8}$$

$$u\frac{\partial\theta}{\partial X}=\frac{\alpha_{nf}}{\alpha_f}\frac{\partial^2\theta}{\partial Y^2}, \tag{9}$$

其边界条件为

$$U(0)=U(L)=0,-\left.\frac{\partial\theta}{\partial Y}\right|_{Y=0}=\left.\frac{\partial\theta}{\partial Y}\right|_{Y=L}=1, \tag{10}$$

以及质量守恒关系为

表 1 纳米颗粒与基液的热物理性质

Table 1 Thermophysical properties of nanoparticles and the base fluid

物理性质	Cu	Al_2O_3	TiO_2	基液(水)
比热容系数c_p/(J/kgK)	385	765	686.2	4179
密度ρ/(kg/m^3)	8933	3970	4250	997.1
导热系数k/(W/mK)	400	40	8.9538	0.613
热扩散系数$\alpha/10^7$(m^2/s)	11163.1	131.7	30.7	1.47
热膨胀系数$\beta/10^{-5}$(1/K)	1.67	0.85	0.9	21

$$\int_0^1 U\mathrm{d}Y=1. \tag{11}$$

其中 $P_1=Gr\sin\gamma/Re$ 和 $P_2=Gr\cos\gamma/\left(Re^2Pr\right)$ 是无量纲压力参数，$Gr=g\beta_f qL^4/\left(k_f\nu_f{}^2\right)$ 是格拉晓夫数，$Re=\bar{u}L/\nu_f$是雷诺数。

假设纳米流体中的基液和纳米颗粒处于热平衡状态，没有相对滑移速度。纳米流体在倾斜通道中做混合对流运动，且纳米流体为不可压缩流体。表 1 给出了基液(水)和纳米颗粒的热物性参数[56]。纳米流体的有效密度，比热容，动力黏度和热扩散系数[57–58]由以下公式计算

$$\rho_{nf}=(1-\phi)\rho_f+\phi(\rho\beta)_n, \tag{12}$$

$$(\rho c_p)_{nf}=(1-\phi)(\rho c_p)_f+\phi(\rho c_p)_n, \tag{13}$$

$$\mu_{nf}=\mu_f/(1-\phi)^{2.5}, \tag{14}$$

$$\alpha_{nf}=k_{nf}/(\rho c_p)_{nf}. \tag{15}$$

纳米流体导热系数采用由HAMILTON等[59]提出的公式计算

$$\frac{k_{nf}}{k_f}=\frac{k_n+(n-1)k_f-(n-1)\phi(k_f-k_n)}{k_n+(n-1)k_f+\phi(k_f-k_n)}, \tag{16}$$

式中，下标f代表基液，nf代表纳米流体；ϕ为纳米颗粒体积分数；n为纳米颗粒形状因子，$n=3/\psi$，ψ为纳米颗粒球形度。当纳米颗粒形状为柱状、立方体形和球形，等效球径dp=45 nm时，其球形度分别为0.52，0.81 和 1.0，如图 3 所示。

考虑边界条件(10)，使用软件MATHEMATICA解

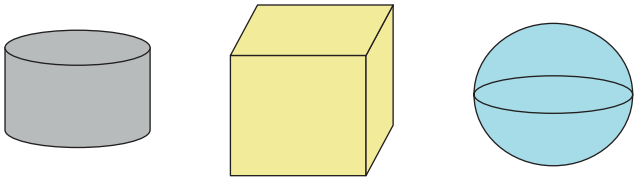

图 3 不同形状的纳米颗粒

Fig. 3 Different shapes of nanoparticle

析求解得到速度分布U，温度分布θ和压力分布P为

$$\begin{aligned}U(Y)=&a\left[\sinh(mY)+\sin(mY)\right]+\\&b\left[\cosh(mY)-\cos(mY)\right]+c\sin(mY),\end{aligned} \tag{17}$$

$$\begin{aligned}\theta(X,Y)=&\frac{2}{m^2}\left\{a\left[\sinh(mY)-\sin(mY)\right]+\right.\\&\left.b\left[\cosh(mY)+\cos(mY)\right]-c\sin(mY)\right\}-\\&\frac{2P_2}{P_1}\frac{\alpha_{nf}}{\alpha_f}Y+2\frac{\alpha_{nf}}{\alpha_f}X+A,\end{aligned} \tag{18}$$

$$\begin{aligned}P(X,Y)=&\frac{(\rho\beta)_{nf}}{(\rho\beta)_f}\left\{\frac{2P_2}{m^3}\left[a\left(\cosh(mY)+\cos(mY)\right)\right.\right.,\\&\left.+b\left(\sinh(mY)+\sin(mY)\right)+c\cos(mY)\right]\\&+P_2\left(2\frac{\alpha_{nf}}{\alpha_f}XY+AY-\frac{P_2}{P_1}\frac{\alpha_{nf}}{\alpha_f}Y^2\right)\\&-P_1\left(AX+\frac{\alpha_{nf}}{\alpha_f}X^2\right)\end{aligned} \tag{19}$$

其中A和B是常数，其值取决于P_1和P_2的给定值，并且它们必须满足θ和P。参数a、b、c和m分别为

$$\begin{aligned}a=&\frac{\left[m-c+c\cos(m)\right]\left[\cosh(m)-\cos(m)\right]}{-2\left[\cosh(m)\cos(m)-1\right]}\\&+\frac{c\sin(m)\left[\sinh(m)-\sin(m)\right]}{-2\left[\cosh(m)\cos(m)-1\right]}\\&+\frac{c\sin(m)\left[\cosh(m)-\cos(m)\right]}{2\left[\cosh(m)\cos(m)-1\right]}\end{aligned}$$

$$c=m\left(\frac{1}{2}-\frac{P_2}{P_1}\frac{\alpha_{nf}}{\alpha_f}\right),m^4=2P_1\frac{(\rho\beta)_{nf}}{(\rho\beta)_f}\frac{\mu_{nf}}{\mu_f}, \tag{20}$$

当P_1和P_2的值给定时，U, θ和P的解析解则完全可以确定。注意，水平情况(P_1=0)的解析解，可以通过在m较小时将上述解展开得到，或者更简单地，通过设置P_1=0 来求解方程(7)–(9)。当纳米颗粒体积分数ϕ=0时，则解还原为文献LAVINE[49]的解。在这个问题中，实际感兴趣的物理量是壁面摩擦系数$C_f Re$和努赛尔数Nu，由下式给出

$$C_f Re=\frac{\tau_w}{\frac{1}{2}\rho_f\bar{u}^2}\frac{\bar{u}L}{\nu_f},Nu=\frac{2qL}{k_f(T_w-T_b)}, \tag{21}$$

$$\tau_w=\pm\mu_{nf}\left.\frac{\partial u}{\partial y}\right|_{y=0,L}, \tag{22}$$

其中 ± 符号分别对应于下壁面和上壁面。

将式(6)和式(22)代入式(21)，得到

当Y=0 时，$C_f Re=2m\frac{\mu_{nf}}{\mu_f}(2a+c)$，

当 $Y=1$ 时，

$$C_f Re = -2m\frac{\mu_{nf}}{\mu_f}\left\{a\left[\cosh(m)+\cos(m)\right]+b\left[\sinh(m)+\sin(m)\right]+c\cos(m)\right\}. \quad (23)$$

壁面平均摩擦系数由以下公式得出：

$$\overline{C_f Re} = \frac{1}{2}\left[C_f Re(Y=0)+C_f Re(Y=1)\right] = \frac{\mu_{nf}}{\mu_f}\frac{m^2\left[\cos(m)-\cosh(m)-\sin(m)\sinh(m)\right]}{\cos(m)\cosh(m)-1}. \quad (24)$$

无量纲局部努塞尔数 Nu 和平均努塞尔数 $\overline{Nu}$，分别定义如下：

$$Nu = \frac{2qL}{k_f(T_w-T_b)} = \frac{2}{\theta_w-\theta_b}, \quad (25)$$

$$\overline{Nu} = \frac{1}{L}\int_0^L Nu\,\mathrm{d}X. \quad (26)$$

其中

$$\theta_b = \int_0^1 U\theta\,\mathrm{d}Y, \theta_w = \theta(Y=0,1). \quad (27)$$

3 计算结果与讨论

为了研究不同纳米颗粒球形度 ψ 和纳米颗粒体积分数 ϕ 对流体流动和传热的基本参数的影响，例如压力参数 P_1，P_2，速度分布 U，温度分布 $\theta-\theta_b$，壁面平均摩擦系数 $\overline{C_f Re}$，平均努塞尔数 $\overline{Nu}$，进行如下图表分析讨论。流动逆转发生在上壁面满足 $(\mathrm{d}U/\mathrm{d}Y)|_{Y=1}=0$，或者 $C_f Re\,|_{Y=1}=0$。基于等式(22)的 P_1 和 P_2 的约束关系可以得到

$$\frac{\alpha_{nf}}{\alpha_f}P_2 = \frac{P_1}{2}\frac{\cos(m)-\cosh(m)-\sin(m)\sinh(m)}{\cos(m)-\cosh(m)+\sin(m)\sinh(m)}. \quad (28)$$

不同纳米颗粒球形度 ψ 和纳米颗粒体积分数 ϕ 条件下的基础流体(H_2O)和纳米流体($Cu\text{-}H_2O$)的流动状态图，每条曲线都存在弯曲，对应于 $P_2=0$ 并且 $P_1=P_{1,c}$，如表 2 和图 4，5 所示。$P_{1,c}$ 是 P_1 的临界值，当 $\phi=0$ 时，该值为 250.28，与文献 LAVINE[49] 数据吻合，验证了计算程序的准确性和可靠性。随着纳米颗粒体积分数 ϕ 增大，临界值 $P_{1,c}$ 同时增大，而 $Cu\text{-}H_2O$ 纳米流体的临界值 $P_{2,c}$ 基本保持不变，$Al_2O_3\text{-}H_2O$ 和 $TiO_2\text{-}H_2O$ 纳米流体的临界值 $P_{2,c}$ 也相应增大。以 $P_{1,c}$ 值作垂线，将所涉及的流动区域分为两部分。当 $P_1 \leqslant P_{1,c}$ 时，该曲线上半部分是只在上壁面发生逆流的区域，下半部分是不可能发生逆流的区域。当 $P_1 \geqslant P_{1,c}$ 时，该曲线将发生流动逆转的状态与仅下壁面流动逆转状态分开。计算结果表明，纳米颗粒的体积分数 ϕ 在延迟逆流发生方面起着关键作用。纳米流体比基础流体具有更大的延迟范围，约为基础流体的 2.2 倍。另一方面，随着纳米颗粒球形度 ψ 增大，P_2 值也相应增大。随着纳米颗粒的体积分数 ϕ 从 0.05 增大到 1.0 时，不同纳米颗粒球形度的影响明显增强。

基液和纳米流体的速度分布如图 6−8 所示，分

表 2 P_1 和 P_2 的临界值(ψ=1.0)

Table 2 The critical values of P_1 and P_2 (ψ=1.0)

临界值	类型	ϕ=0	ϕ=0.05	ϕ=0.1
$P_{1,c}$	H_2O[49]	250.28	–	–
	$Cu\text{-}H_2O$	250.28	288.67	335.34
	$Al_2O_3\text{-}H_2O$	250.28	296.98	355.52
	$TiO_2\text{-}H_2O$	250.28	296.65	354.69
$P_{2,c}$	H_2O[49]	35.99	–	–
	$Cu\text{-}H_2O$	35.99	35.54	35.56
	$Al_2O_3\text{-}H_2O$	35.99	36.59	37.75
	$TiO_2\text{-}H_2O$	35.99	37.58	39.04

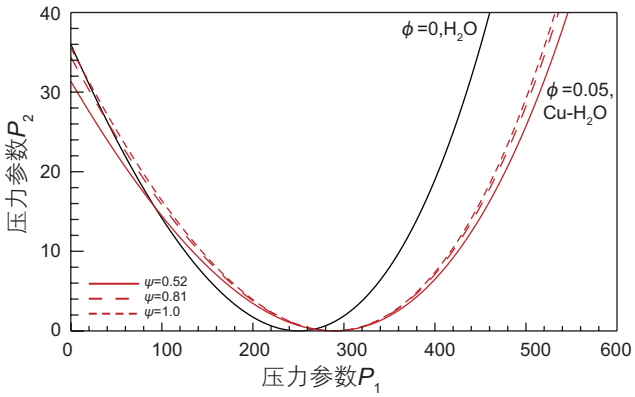

图 4 基液和纳米流体的流态图(ϕ=0.05)

Fig. 4 Flow regime map of the base fluid and nanofluid (ϕ=0.05)

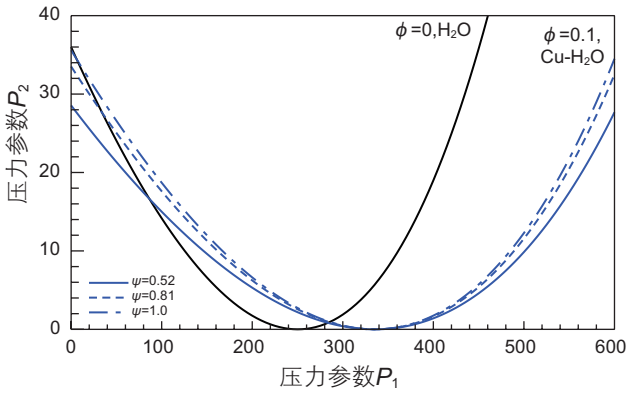

图 5 基液和纳米流体的流态图(ϕ=0.1)

Fig. 5 Flow regime map of the base fluid and nanofluid (ϕ=0.1)

析了当P_1=100，P_2 分别为 0 和 36 时不同纳米颗粒球形度ψ和纳米颗粒体积分数ϕ条件下的基液和纳米流体的速度分布。当P_1=100，P_2=0 时，在中心线附近区域，随着纳米颗粒体积分数ϕ的增大，纳米流体速度U减小。在靠近两壁面(Y=0,1)附近，随着ϕ的增加，纳米流体速度U也增加。计算结果表明，与基液相比纳米流体延迟了上下壁面附近的速度降低。在P_1=100，P_2=36 的情况下，随着纳米颗粒球形度ψ的增加，在下壁面(Y=0)附近，速度峰值降低；而在上壁面(Y=1)附近的速度随流动反转而减小。同时随着纳米颗粒体积分数ϕ的增大，速度变化明显增强。

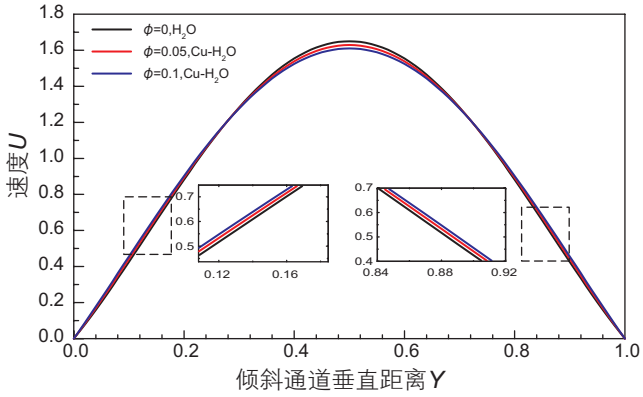

图 6　基液和纳米流体的速度分布 (P_2=0, P_1=100)

Fig. 6　The velocity profiles for the base fluid and nanofluid (P_2=0, P_1=100)

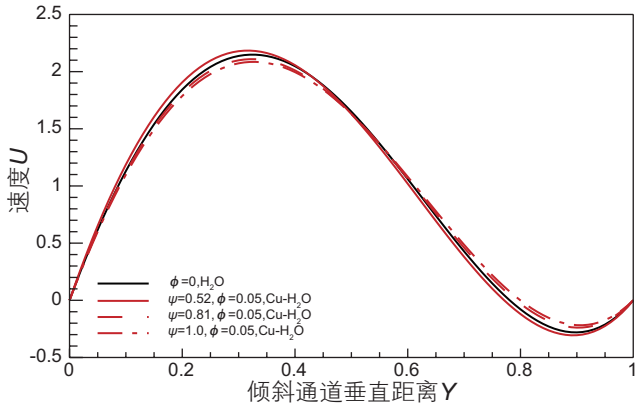

图 7　基液和纳米流体的速度分布 (P_2=36, P_1=100, ϕ=0.05)

Fig. 7　The velocity profiles for the base fluid andnanofluid (P_2=36, P_1=100, ϕ=0.05)

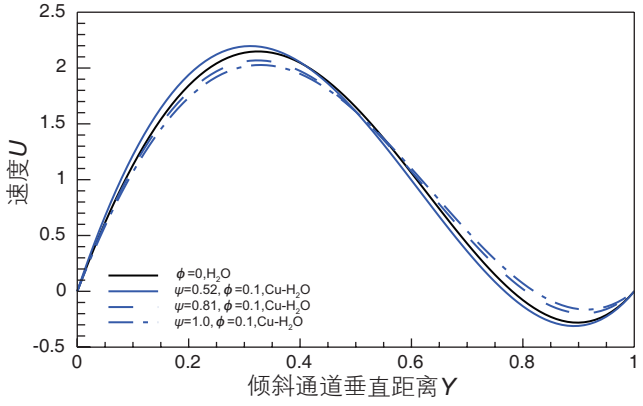

图 8　基液和纳米流体的速度分布 (P_2=36, P_1=100, ϕ=0.1)

Fig. 8　The velocity profiles for the base fluid andnanofluid (P_2=36, P_1=100, ϕ=0.1)

基液和纳米流体的温度分布如图 9，10 所示，分析了当P_1=100，P_2 分别取 0 和 36 时基础流体和纳米流体的温度分布，温度函数采用$\theta-\theta_b$，消除了对x的依赖性。随着P_2 的增大，上壁面附近的温度也相应升高。同时，温度谷向下壁面移动，其值随P_2 的增加而不断增大，然而下壁面附近的温度几乎不变。随着纳

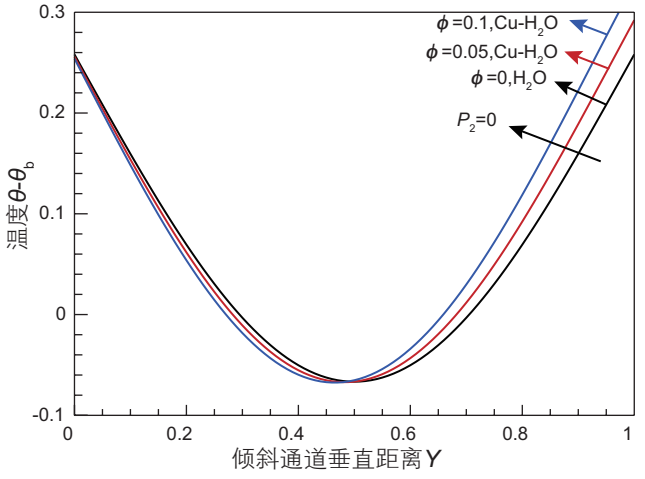

图 9　基液和纳米流体的温度分布 (P_2=0, P_1=100)

Fig. 9　The temperature profiles for the base fluid and nanofluid (P_2=0, P_1=100)

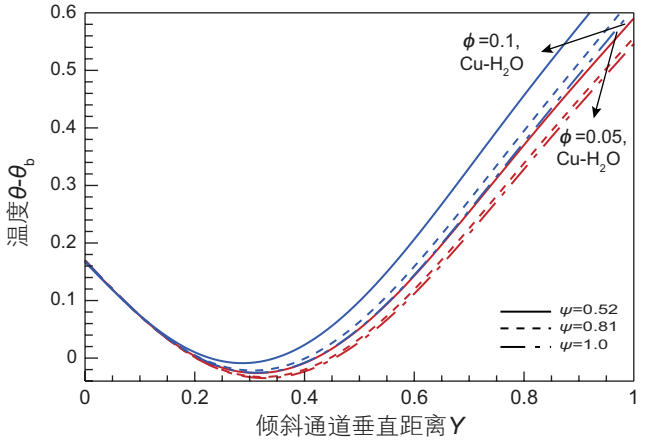

图 10　纳米流体的温度分布 (P_2=36, P_1=100)

Fig. 10　The temperature profiles for the nanofluid (P_2=36, P_1=100)

米颗粒的体积分数ϕ的增大，上壁面附近的温度变化越来越大。随着纳米颗粒球形度ψ的增加，壁面温度降低；同时，随着纳米颗粒的体积分数ϕ的增大，纳米颗粒球形度的对于降低壁面温度的影响增强。当ϕ=0.05，ψ=0.52 或者ϕ=0.1，ψ=1.0 的温度函数$\theta-\theta_b$的值比较接近。

壁面平均摩擦系数$\overline{C_f Re}$和平均努塞尔数$\overline{Nu}$是实际感兴趣的物理量，如图 11−13 所示。图 11 显示了随着纳米颗粒的体积分数ϕ增大，纳米流体的壁面平均摩擦系数$\overline{C_f Re}$也增大，而且与纳米颗粒球形度ψ和无量纲压力参数P_2均无关，随着P_1的增大而单调减小。与基液相比，纳米流体的壁面平均摩擦系数$\overline{C_f Re}$，在下壁面(Y=0)处增加 30%(ϕ=0.05 或 1)，在上壁面(Y=1)处的增加 4.5%(ϕ=0.05)，33%(ϕ=0.1)。图 12，13 显示了纳米颗粒球形度ψ和纳米颗粒体积分数ϕ对基液和纳米流体的平均努塞尔数$\overline{Nu}$的影响。与平均摩擦系数相反，平均努塞尔数与纳米颗粒球形度ψ，纳米颗粒的体积分数ϕ和无量纲压力参数P_2均有关。当P_2=0 时，随着P_1的增加，基液和纳米流体的平均努塞尔数单调增加。当P_2=0，P_1=600 时，与基液相比，纳米流体的平均努塞尔数$\overline{Nu}$增加 8.7%(ϕ=0.05)，19.1%(ϕ=0.1)。如图 13 所示，随着纳米颗粒体积分数ϕ的增大，平均努塞尔数谷向下壁面移动，其值随P_2的增大而连续增大。随着纳米颗粒球形度ψ的增大，平均努塞尔数值也增大。显然，与基液相比，纳米流体具有更好的热物理性质和传热性能。

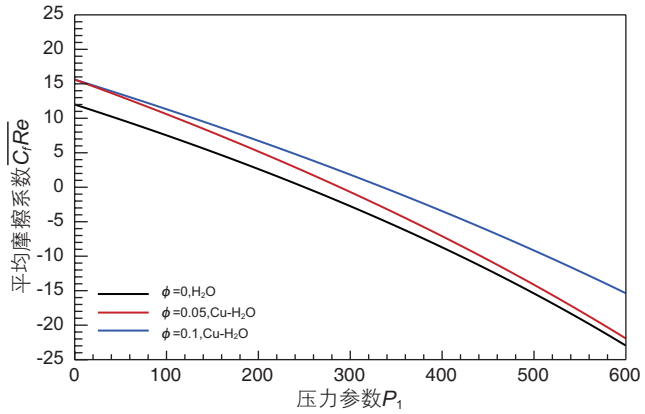

图 11 平均摩擦系数$\overline{C_f Re}$随P_1的变化

Fig. 11 Variation of average $C_f Re$ with P_1

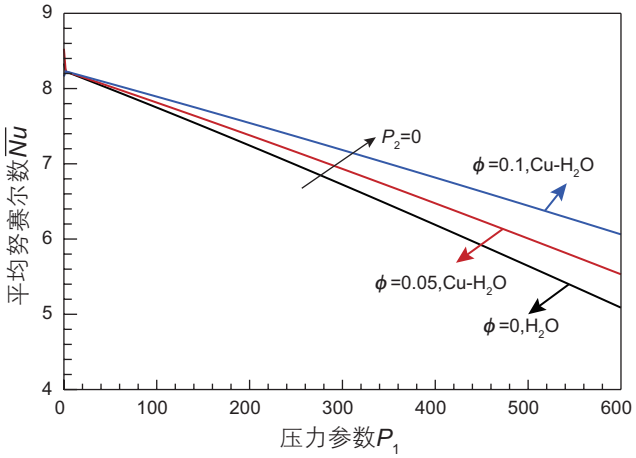

图 12 当P_2=0 时平均努赛尔数$\overline{Nu}$随P_1的变化

Fig. 12 Variation of average Nu with P_1 for P_2 = 0

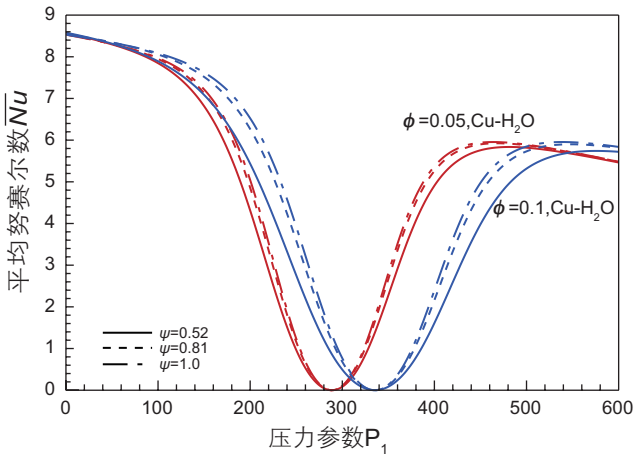

图 13 当P_2=36 时平均努赛尔数$\overline{Nu}$随P_1的变化

Fig. 13 Variation of average Nu with P_1 for P_2 = 36

4 结论

本文对纳米微球在石油工程提高采收率中的应用进行了梳理和分析，深入研究纳米颗粒在倾斜通道中反向混合对流的传输机理，研究不同纳米颗粒球形度和纳米颗粒体积分数对流体流动和传热的物理参数的影响，可为后续提高采收率纳米微球的参数微调提供

理论支撑。本文主要结论如下：

(1)纳米颗粒的体积分数ϕ在延迟逆流发生方面起着关键作用。纳米流体比基础流体具有更大的延迟范围，约为基础流体的2.2倍。同时，随着纳米颗粒球形度ψ增大，P_2值也相应增大。

(2)纳米颗粒体积分数ϕ对速度和温度分布的影响是明显的，随着ϕ的增大，与基液相比纳米流体延迟了上下壁面附近的速度降低。同时，随着纳米颗粒球形度ψ的增大，壁面温度降低。

(3)随着纳米颗粒的体积分数ϕ增大，纳米流体的壁面平均摩擦系数$\overline{C_f Re}$也增大，而且与纳米颗粒球形度ψ和无量纲压力参数P_2均无关，随着P_1的增大而单调减小。

(4)平均努塞尔数$\overline{Nu}$与纳米颗粒球形度ψ，纳米颗粒的体积分数ϕ和无量纲压力参数P_2均有关。随着纳米颗粒球形度ψ的增大，平均努塞尔数值也增大。

参考文献

[1] CHOI S, EASTMAN J A. Enhancing thermal conductivity of fluids with nanoparticles[J]. ASME International Mechanical Engineering Congress & Exposition, 1995, 66: 99−105.

[2] 郑俨钊, 雷建永, 王桥, 等. 纳米流体研究综述[J]. 当代化工, 2021, 50(3): 724−728. [ZHENG Y Z, LEI J Y, WANG Q, et al. Summary of nanofluid research[J]. Contemporary Chemical Industry, 2021, 50(3): 724−728.]

[3] 佘跃惠, 曾琦, 董浩, 等. 纳米材料改变岩石矿物润湿性的研究进展[J]. 科学技术与工程, 2021, 21(8): 2997−3005. [SHE Y H, ZENG Q, DONG H. Development of changing rock mineral wettability with nanomaterials[J]. Science Technology and Engineering, 2021, 21(8): 2997−3005.]

[4] DRUETTA P, PICCHIONI F. Polymer and nanoparticles flooding as a new method for enhanced oil recovery[J]. Journal of Petroleum Science and Engineering, 2019, 177: 479−495.

[5] 田进, 何淼, 王晓亮. 纳米粒子在钻完井中的应用现状[J]. 应用化工, 2021, 50(1): 152−154. [TIAN J, HE M, WANG X L. Application status of nanoparticles in drilling and completion[J]. Applied Chemical Industry, 2021, 50(1): 152−154.]

[6] MOHEBBIFAR M, GHAZANFARI M H, VOSSOUGHI M. Experimental investigation of nano-biomaterial applications for heavy oil recovery in shaly porous models: a pore-level study[J]. Journal of Energy Resources Technology, 2015, 137: 014501.

[7] ESFE M H, HOSSEINIZADEH E, ESFANDEH S. Flooding numerical simulation of heterogeneous oil reservoir using different nanoscale colloidal solutions[J]. Journal of Molecular Liquids, 2020, 302: 111972.

[8] 李俊键, 苏航, 姜汉桥, 等. 微流控模型在油气田开发中的应用[J]. 石油科学通报, 2018, 3(3): 284−301. [LI J J, SU H, JIANG H Q, et al. Application of microfluidic models in oil and gas field development[J]. Petroleum Science Bulletin, 2018, 3(3): 284−301.]

[9] 席洋洋, 高玉国, 司爱国. 杂化纳米流体的制备及热导率研究[J]. 汽车实用技术, 2019, 5: 147−149. [XI Y Y, GAO Y G, SI A G. Preparation and thermal conductivity of hybrid nanofluids[J]. Automobile applied technology, 2019, 5: 147−149.]

[10] JALAL M, MANSOURI E, SHARIFPOUR M, et al. Mechanical, rheological, durability and microstructural properties of high performance self-compacting concrete containing SiO_2 micro and nanoparticles[J]. Materials & Design, 2012, 34: 389−400.

[11] SHIH J, CHANG T, HSIAO T. Effect of nanosilica on characterization of Portland cement composite[J]. Materials Science and Engineering: A, 2006, 424(1–2): 266−274.

[12] PANG X, BOUL P J, CUELLO JIMENEZ W. Nanosilicas as accelerators in oil well cementing at low temperatures[J]. SPE Drilling and Completion, 2014, 29(1): 98−105.

[13] FAKOYA M F, SHAH S N. Effect of silica nanoparticles on the rheological properties and filtration performance of surfactant-based and polymeric fracturing fluids and their blends[J]. SPE Drilling and Completion, 2018, 33(02): 100−114.

[14] ISMAIL A R, AFTAB A, IBUPOTO Z H, et al. The novel approach for the enhancement of rheological properties of water-based drilling fluids by using multi-walled carbon nanotube, nano-silica and glass beads[J]. Journal of Petroleum Science and Engineering, 2016, 139: 264−275.

[15] YANG X, SHANG Z, LIU H, et al. Environmental-friendly salt water mud with nano-SiO_2 in horizontal drilling for shale gas[J]. Journal of Petroleum Science and Engineering, 2017, 156: 408−418.

[16] ABDULLAHI M B, RAJAEI K, JUNIN R, et al. Appraising the impact of metal-oxide nanoparticles on rheological properties of HPAM in different electrolyte solutions for enhanced oil recovery[J]. Journal of Petroleum Science and Engineering, 2019, 172: 1057−1068.

[17] ALSABA M T, DUSHAISHI M F A, ABBAS A K. A comprehensive review of nanoparticles applications in the oil and gas industry[J]. Journal of Petroleum Exploration and Production Technology, 2020, 10: 1389−1399.

[18] 吴天江, 郑明科, 周志平, 等. 低渗透油藏纳米微球调驱剂封堵性评价新方法[J]. 断块油气田, 2018, 25(4): 498−501. [WU T J, ZHENG M K, ZHOU Z P. New method for plugging performance evaluation of polymeric nanospheres in low permeability reservoir[J].

Fault-block oil & gas field, 2018, 25(4): 498−501.]

[19] 沙鹏. 新型聚合物复合纳米微球调剖驱油剂研究[J]. 石油化工高等学校学报, 2020, 33(5): 54−58. [SHA P. Study on a new polymer composite nano-microsphere for profile control and oil displacement[J]. Journal of petrochemical universities, 2020, 33(5): 54−58.]

[20] 康万利, 周博博, 杨红斌, 等. 油田调驱用聚合物微球的研究进展[J]. 高分子材料科学与工程, 2020, 36(9): 173−180. [KANG W L, ZHOU B B, YANG H B, et al. Comprehensive review of polymer microspheres for oil field conformance control and flooding[J]. Polymer materials science and engineering, 2020, 36(9): 173−180.]

[21] YAO C, LEI G, LI L, et al. Selectivity of pore-scale elastic microspheres as a novel profile control and oil displacement agent[J]. Energy & Fuels, 2012, 26(8): 5092−5101.

[22] MAURYA N K, KUSHWAHA P, MANDAL A. Studies on interfacial and rheological properties of water soluble polymer grafted nanoparticle for application in enhanced oil recovery[J]. Journal of the Taiwan Institute of Chemical Engineers, 2017, 70: 319−330.

[23] 冯全宏, 屈策计, 张伟, 等. 一种聚合物纳米微球调驱剂的制备及性能评价[J]. 辽宁石油化工大学学报, 2019, 39(4): 24−27. [FENG Q H, QU C J, ZHANG W, et al. Preparation and performance evaluation of a polymer nanospheres control and flooding agent [J]. Journal of Liaoning Shihua University, 2019, 39(4): 24−27.]

[24] WENHAO D, PENGWEI W, ZHIXIN Z, et al. Facile preparation and characterization of temperature-responsive hydrophilic cross−linked polymer microspheres by aqueous dispersion polymerization[J]. European Polymer Journal, 2020, 128: 109610.

[25] HAROUN M, HASSAN S A, ANSARI A, et al. Smart nano-EOR process for Abu Dhabi carbonate reservoirs[J]. Society of Petroleum Engineers, 2012, 162386: 1−13.

[26] HENDRANINGRAT L, TORSATER O. Metal oxide-based nanoparticles: revealing their potential to enhance oil recovery in different wettability systems[J]. Applied Nanoscience, 2015, 5 (2): 181−199.

[27] HUANG T, EVANS B A, CREWS J B, et al. Field case study on formation fines control with nanoparticles in offshore applications[J]. Society of Petroleum Engineers, 2010, 135088: 1−8.

[28] 陈渊, 孙玉青, 李飞鹏, 等. 纳米微球深部调驱技术在河南油田的应用[J]. 石油钻采工艺, 2012, 34(3): 87−90. [CHEN Y, SUN Y Q, LI F P. Application of nanosphere deep profile control and displacement technology in He'nan oilfield[J]. Oil drilling & production technology, 2012, 34(3): 87−90.]

[29] 贾玉琴, 郑明科, 杨海恩, 等. 长庆油田低渗透油藏聚合物微球深部调驱工艺参数优化[J]. 石油钻探技术, 2018, 46(1): 75−82. [JIA Y Q, ZHENG M K, YANG H E. Optimization of operational parameters for deep displacement involving polymer microspheres in low permeability reservoirs of the Changqing oilfield[J]. Petroleum drilling techniques, 2018, 46(1): 75−82.]

[30] 周海燕, 刘斌, 孙强, 等. 海上河流相稠油油田纳米微球多轮次调驱效果评价研究[J]. 新疆石油天然气, 2021, 17(1): 60−64. [ZHOU H Y, LIU B, SUN Q, et al. Study on the effect evaluation of nanoscale microsphere multi-wheel drive in offshore fluvial heavy oil field[J]. Xinjiang Oil & Gas, 2021, 17(1): 60−64.]

[31] ESFE M H, SAEDODIN S, BIGLARI M, et al. Experimental investigation of thermal conductivity of CNTs-Al_2O_3/water: A statistical approach[J]. International Communications in Heat Mass Transfer, 2015, 69: 29−33.

[32] ABEROUMAND S, JAFARIMOGHADDAM A, MORAVEJ M, et al. Experimental study on the rheological behavior of silver-heat transfer oil nanofluid and suggesting two empirical based correlations for thermal conductivity and viscosity of oil based nanofluids[J]. Applied Thermal Engineering, 2016, 101: 362−372.

[33] YANG L, XU J, DU K, et al. Recent developments on viscosity and thermal conductivity of nanofluids[J]. Powder Technology, 2017, 317: 348−369.

[34] PRAMUANJAROENKIJ A, TONGKRATOKE A, KAKA S. Numerical study of mixing thermal conductivity models for nanofluid heat transfer enhancement[J]. Journal of Engineering Physics and Thermophysics, 2018, 91: 104−114.

[35] ESFE M H. On the evaluation of the dynamic viscosity of non-Newtonian oil based nanofluids[J]. Journal of Thermal Analysis and Calorimetry, 2019, 135: 97−109.

[36] CHANG T S, LIN T F. Steady and oscillatory opposing mixed convection in a symmetrically heated vertical channel with a low-Prandtl number fluid[J]. International Communications in Heat Mass Transfer, 1993, 36: 3783−3795.

[37] BARLETTA A. Dual mixed convection flows in a vertical channel[J]. International Communications in Heat Mass Transfer, 2005, 48: 4835−4845.

[38] CHANG T S. Effects of a finite section with linearly varying wall temperature on mixed convection in a vertical channel[J]. International Communications in Heat Mass Transfer, 2007, 50: 2346−2354.

[39] XU H, POP I. Fully developed mixed convection flow in a vertical channel filled with nanofluids[J]. International Communications in Heat Mass Transfer, 2012, 39: 1086−1092.

[40] JAMALUDIN A, NAGANTHRAN K, NAZAR R, et al. MHD mixed convection stagnation-point flow of Cu-Al_2O_3/water hybrid nanofluid over a permeable stretching/shrinking surface with heat source/sink[J]. European Journal of Mechanics − B/Fluids, 2020, 84: 71−80.

[41] BIANCO V, CHIACCHIO F, MANCA O, et al. Numerical investigation of nanofluids forced convection in circular tubes[J]. Applied Thermal Engineering, 2009, 29: 3632−3642.

[42] ESFE M H, ARANI A A A, AZIZI T, et al. Numerical study of laminar-forced convection of Al_2O_3−water nanofluids between two parallel plates[J]. Journal of Mechanical Science Technology, 2017, 31(2): 785−796.

[43] 陈彦君, 李元阳, 刘振华. 基于多相流模型的纳米流体在水平细圆管内强制对流换热数值模拟[J]. 上海交通大学学报, 2014, 48(9): 1303−1308. [CHEN Y J, LI Y Y, LIU Z H. Numerical simulation of forced convective heat transfer and flow characteristics of nanofluids in small tubes using multiphase models[J]. Journal of Shanghai Jiao Tong University, 2014, 48(9): 1303−1308.]

[44] 白国君, 王刚, 马兵善, 等. 变物性参数对微通道内纳米流体强制对流换热的影响[J]. 工程热物理学报, 2018, 39(2): 389−394. [BAI G J, WANG G, MA B S, et al. Effect of variable thermophysical properties on forced convection heat transfer of nanofluid in microchannel[J]. Journal of Engineering Thermophysics, 2018, 39(2): 389−394.]

[45] 王刚, 张倩马, 兵善. 纳米颗粒球形度对平板通道中Al_2O_3 ─水纳米流体强制对流换热的影响[J]. 兰州理工大学学报, 2021, 47(1) : 62−65. [WANG G, ZHANG Q, MA B S. Effect of sphericity of nanoparticles on forced convection heat transfer of Al_2O_3−water nanofluid in parallel-plate channel[J]. Journal of Lanzhou University of Technology, 2021, 47(1): 62−65.]

[46] CHEIN R, CHUANG J. Experimental microchannel heat sink performance studies using nanofluids[J]. International Journal of Thermal Sciences, 2007, 46(1): 57−66.

[47] GOHARKHAH M, ASHJAEE M, SHAHABADI M. Experimental investigation on convective heat transfer and hydrodynamic characteristics of magnetite nanofluid under the influence of an alternating magnetic field[J]. International Journal of Thermal Sciences, 2016, 99: 113−124.

[48] HO C J, CHANG C Y, YAN W M, et al. A combined numerical and experimental study on the forced convection of Al_2O_3−water nanofluid in a circular tube[J]. International Communications in Heat Mass Transfer, 2018, 120: 66−75.

[49] LAVINE A S. Analysis of fully developed opposing mixed convection between inclined parallel plates[J]. Heat Mass Transfer, 1988, 23: 249−257.

[50] BARLETTA A, ZANCHINI E. Mixed convection with viscous dissipation in an inclined channel with prescribed wall temperatures[J]. International Communications in Heat Mass Transfer, 2001, 44: 4267−4275.

[51] AYDIN O, KAYA A. MHD mixed convective heat transfer flow about an inclined plate[J]. Heat Mass Transfer, 2009, 46: 129−136.

[52] CIMPEAN D S, POP I. Fully developed mixed convection flow of a nanofluid through an inclined channel filled with a porous medi−um[J]. International Communications in Heat Mass Transfer, 2012, 55: 907−914.

[53] GOYAL M, BHARGAVA R. Simulation of natural convective boundary layer flow of a nanofluid past a convectively heated inclined plate in the presence of magnetic field[J]. International Journal of Applied and Computational Mathematics, 2018, 4: 63.

[54] KHADEMI R, RAZMINIA A, SHIRYAEV V I. Conjugate-mixed convection of nanofluid flow over an inclined flat plate in porous media[J]. Applied Mathematics and Computation, 2020, 366: 124761.

[55] YOU X C, LI S Y. Fully developed opposing mixed convection flow in the inclined channel filled with a hybrid nanofluid[J]. Nanoma−terials 2021, 11(5): 1107.

[56] OZTOP H F, ABU-NADA E. Numerical study of natural convection in partially heated rectangular enclosures filled with nanofluids[J]. International Journal of Heat and Fluid Flow, 2008, 29: 1326−1336.

[57] BRINKMAN H C. The viscosity of concentrated suspensions and solutions[J]. The Journal of Chemical Physics, 1952, 20: 571−581.

[58] MAIGA S E B, PALM S J, NGUYEN C T, et al. Heat transfer enhancement by using nanofluids in forced convection flows[J]. Interna−tional Journal of Heat and Fluid Flow, 2005, 26: 530−546.

[59] HAMILTON R L, CROSSER O K. Thermal conductivity of heterogeneous two-component systems[J]. Industrial and Engineering Chemistry Fundamentals, 1962, 1(3): 187−191.

(责任编辑　林伯韬　编辑　马桂霞)